Quercetin/oleic acid-based G-protein-coupled receptor 40 ligands as new insulin secretion modulators

Future Medicinal Chemistry

Quercetin/Oleic Acid-Based Hybrid Molecules as New Insulin Output Modulators

Journal:	*Future Medicinal Chemistry*
Manuscript ID	FMC-2017-0113
Manuscript Type:	Research Article
Keywords:	GPR40 Molecular Docking, Antidiabetic Drugs, Quercetin/Oleic Acid-Based Hybrid Molecules

Quercetin/Oleic Acid-Based Hybrid Molecules as New Insulin Output Modulators

Abstract

Background: Management of Type 2 Diabetes Mellitus (T2DM) by diet is achievable at the early stage of the disease; patients usually underestimate this approach and an appropriate drug therapy is required. Anyway, antidiabetic agents have both undesirable and severe side effects.

Results: Starting from quercetin and olive oil, that have effect on insulin secretion, a small set of hybrid molecules was synthetized. Insulin secretion was evaluated in both *in vitro* and *ex-vivo* models. **AV1** was able to enhance insulin output dose-dependently, behaving as a conceivable agonist of GPR40.

Conclusions: AV1 represents an interesting tool which interacts with GPR40. Further studies will be carried out to evaluate the exact binding mode, and also to enlarge the library of these anti-diabetic agents.

Graphical abstract

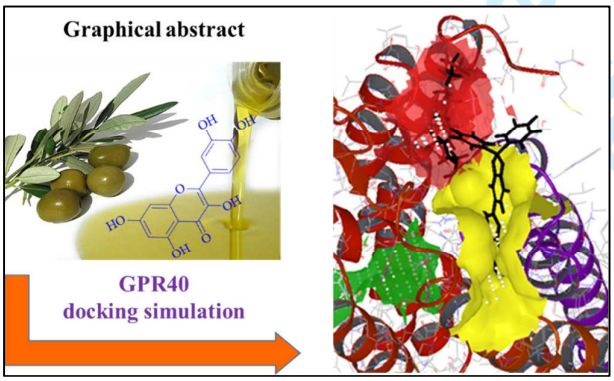

Keywords: GPR40 Molecular Docking, Antidiabetic Drugs, Quercetin/Oleic Acid-Based Hybrid Molecules, Insulin secretion.

Introduction

The high incidence of Type 2 Diabetes Mellitus (T2DM) drives the need for new anti-diabetic therapies more effective and with less side effects.**[1]** Crucial aspects in the pathogenesis of T2DM are the impairment of β-cell mass and the defects in β-cell glucose sensitivity, which in turns affect the Glucose-Stimulated Insulin Secretion (GSIS) from pancreatic β-cells. This latter mechanism is essential to ensure the normal control of blood glucose concentrations.**[2,3]** It is now evident that different G protein-coupled receptors (GPRs) display a role in GSIS, since their activation is able to induce insulin secretion, thus representing a new target. In fact, Fatty Acids (FAs) are physiological

ligands of several GPRs involved in GSIS, such as GPR40, GPR41, GPR43, and GPR120, as well as estrogens, i.e. estradiol, exert their influence through GPR30 activation.**[4-7]** Among natural polyphenolic compounds, Quercetin (3,5,7-trihydroxy-2-(3,4-dihydroxyphenyl)-4*H*-chromen-4-one (Qu) (**Figure 1**) is a GPCRs ligand which shows interesting biological activities including also an important anti-diabetic effect.**[8]** However, its intrinsic poor bioavailability limits the use as dietary supplement for both antioxidant properties and blood glucose managing.**[9,10]** The well-studied receptor that belongs to GPRs family and is able to induce insulin release, as well as incretin secretion by intestinal mucosa (avoiding hypoglycemia risk), is the GPR40. The numerous efforts made over the past decade to develop innovative anti-diabetic drugs that target GPR40 led to the identification of the selective agonist TAK-875. Unfortunately, this compound has failed the phase III of clinical trials due to its liver safety concerns. In fact, TAK-875 showed a severe hepatotoxicity because of a poor metabolism by liver enzyme.**[11]** Very different FAs, in terms of chain length and structural properties, showed an "extraordinarily flat SAR" toward GPR40.**[12]** Experimental and theoretical results provided support for at least three different ligand binding sites on GPR40.**[13-15]** Unfortunately, the exact positioning of such binding sites has not yet been fully understood apart for the cavity able to accommodate the allosteric agonist TAK-875. In effect, the co-crystallization of this ligand within the structure of GPR40 made available the three-dimensional coordinates of its binding pocket.**[13]** Oleic acid is another natural compound, edible and safe, discovered to be a GPR40 ligand.**[16]** Based on this knowledge, our strategy was first to embed the catechol moiety of Qu in a diphenylketal backbone and then to add an oleic side chain at the positions C3 or C3-7, with the aim of driving the hybrid compounds toward GPR40 interaction. The preliminary protection of catechol moiety it is a mandatory condition to guarantee the selective C3 esterification, taking into consideration the reactivity order C4'>C7>C3>C3'>C5 of the Qu hydroxyl groups. Following this rational approach, herein we describe the synthesis and the biological evaluation of two oleic acyl derivatives designed as **AV1** and **AV4**. It is noteworthy that these hybrid molecules could overcome hepatotoxic side effects, because several glucuronidation positions are still available for hepatic metabolism. Biological evaluation of **AV1** and **AV4** was carried out by using the INS-1 832/13 cell line, considered as one of the most physiologically relevant in vitro β-cell models currently available to study human insulin secretion. INS-1 832/13 cells represent a genetically modified INS-1 cell subclone, selected for its robust glucose responsiveness over the physiological range of glucose concentrations (2.8 – 16.7 mM) and because they retain a differentiated cell phenotype over more than six months in culture. These characteristics made INS-1 832/13 cells a widely used tool for studying various aspects of β-cell functions and for the advantageous screening of new compounds.**[17,18]**

Results & Discussion

Chemistry

A simple chemical synthesis was applied to afford acyl derivatives of Qu in a regioselective manner, as depicted in **Figure 2**. Previous paper reported the synthesis of similar compounds, but using hard reaction conditions.**[19]** In particular in our procedure, as first step the catechol group was protected with the double aim of preventing the catechol acylation and excluding the involvement of this moiety in the biological activity. Next, the final oleoyl derivatives were obtained by a conventional condensation reaction, using one equivalent amount of Qu diphenylketal (**AV**) and oleic acid as acyl donor, N,N'-dicyclohexylcarbodiimide (DCC) and dimethylaminopyridine (DMAP) as activator of the carboxyl group and as catalyst, respectively, in dry dichloromethane under inert atmosphere at room temperature in the dark (**Figure 2**). The reaction with an equivalent of oleic acid provided selectively the acyl derivative on **C3**; conversely, two equivalents of fatty acid afforded a double functionalization on **C3-7**. Since the hydroxyl group on **C5** is involved in an hydrogen bound interaction with the **C4** chromen carbonyl, the **C5** substituted derivative has never been isolated. Therefore, **C3** selectivity in comparison to **C7** positions can be achieved just controlling the amount of acylating agent.

Molecular docking of the predicted target

In the attempt to hypothesize the binding mode of quercetin derivatives, the three-dimensional structure of the complex between GPR40 and its allosteric agonist TAK-875 derived from X-ray crystallography**[13]** was used to perform docking calculations. Experimental evidence based on positive functional cooperativity clearly showed that endogenous ligands (such as the docosahexaenoic acid) were able to bind to the orthosteric site, while partial agonists (such as AMG837) and full agonists (such as AMG1638) interacted with two additional and distinct pockets on GPR40.**[12]** Nevertheless, the exact positioning of such binding sites has not yet been elucidated except for the cavity able to accommodate the allosteric agonist TAK-875, whose three-dimensional coordinates are available thanks to the co-crystallization of compound within GPR40 structure.**[13]** The ability of the docking software Glide to reproduce the binding pose of both TAK-875 and the 1-oleoyl-glycerol present on the X-ray structure was preliminarily checked. As a result, orientation of TAK-875 within the allosteric binding site was well reproduced (**Figure 3A**), apart for a reorientation of the terminal sulfonyl edge that is exposed to the solvent and, as a consequence, has a high conformational freedom. In a similar way, the docked oleoyl derivative was placed within

the groove comprised among the transmembrane helixes (TM) 3, 4, and 5, in the same orientation found for the crystallized ligand.

Next, the SiteMap routine was applied to identify potential binding sites on the overall GPR40 structure. As a result, five sites were identified (**Figure 3B**). Two of them corresponded to the pockets that accommodated TAK-875 (site 3, green, **Figure 3B**) and the oleoyl derivative (site 1, gray, **Figure 3B**). An additional site is located just above TM5 and TM6 (site 5, yellow, **Figure 3B** and Figure **4** panel **A**). Moreover, the upper portions of TM1, TM2, and TM7, together with the extracellular loop 1 contributed to define another small pocket (site 4, red, **Figure 3B** and **Figure 4A**). The fifth site was located within the intracellular portion of GPR40 (site 2, magenta, **Figure 3B**). A preliminary visual inspection of these hypothetical binding sites suggested us to discard sites 4 and 5 because of their small size and globular shape not appropriate to accommodate the long alkyl chain of Qu derivatives. However, merging of these two adjacent sites resulted in a cavity where **AV1** could be profitably located (Figure **4** panel **A**). In particular, the alkyl chain of the ligand fulfilled the volume of site 4, while the quercetin moiety was sandwiched between the terminal tail of TM5 and TM6. Importantly, Arg183, which was one of the most important amino acids responsible for anchoring the carboxylic function of GPR40 agonists such as TAK-875,**[12]** also played a fundamental role in stabilizing **AV1** within the cavity. In fact, the terminal guanidine moiety of Arg183 interacted by hydrogen bonds with both the carbonyl and the 5-OH groups of **AV1**. This result led to the hypothesis that such a residue could be interposed between the binding pockets that accommodate TAK-875 and **AV1** (Figure **4** panel **B**). An additional hydrogen bond was found between the 5-OH group of the ligand and a water molecule (HOH2544) interposed between TM5 and TM6. Finally, the diphenyl system protruded from the heptahelical bundle (Figure **4** panel **A**). It is also noteworthy that a potential binding pocket comprised between TM1 and TM7 (that corresponds to the location of site 4) was already hypothesized.**[13]** These considerations suggested that the cavity resulting from merging of site 4 and 5 had size, shape, and functional properties (in terms of lipophilicity and hydrogen bond-acceptor groups) appropriate to made profitable interactions with quercetin derivatives, such as **AV1**. As a consequence, this pocket could represent an additional allosteric binding site for GPR40 agonists.

A depth analysis of site 1 showed a long crevice where the oleoyl-glycerol of the X-ray structure was located (**Figure 5A**). TM4 and TM5 constituted the lateral walls, while TM3 delimited the deepest part of the groove. Close to the cytoplasmic side, the bottom of site 1 also showed a tunnel delimited by basic residues (i.e., Arg37, Arg104, Arg217, Arg218, and Arg221) that could admit to the opposite face of the GPR40 structure, from a region of space comprised between TM4 and TM3 to a region of space comprised between TM7 and TM1 (**Figure 5B**). The alkyl portion of the best

scored docked pose of **AV1** was nearly parallel to TM4 and TM5 and gave extended contacts with the side chains of at least twelve hydrophobic amino acids in the inter-helical space. At the opposite edge of the ligand structure, the terminal quercetin moiety was projected inside the heptahelical bundle. The hydroxyl group at position 5 of the quercetin core gave a bifurcated hydrogen bond with the charged terminal chain of Arg37. An additional hydrogen bond was found between the 7-OH substituent of **AV1** and the guanidinium group of Arg218. Further stabilization of the complex was gained with π-π stacking between one of the phenyl rings of the ketal moiety and the aromatic portion of Phe110. It should be reported that previous studies on GPR40 allosteric sites hypothesized a binding site located between TM4 and TM5.[12] It could represent a route, through the membrane, for the entry of a ligand to site 1, thus giving a certain support for the existence of the same site. On the other hand, the tunnel of site 3 that accommodated TAK-875 was too narrow to admit the quercetin moiety of AV analogues for the interactions with Tyr240, Tyr91, Arg183, and Arg258 described of pivotal importance for anchoring the acidic function of GPR40 agonists. In fact, results of docking simulations performed to check ability of AV1 to bind the allosteric pocket occupied by TAK-875 clearly showed that best docked binding mode of AV1 was characterized by the ligand anchored on the external surface of GPR40. Short dynamics simulations of such complexes showed that the ligand was not able to maintain the pose derived from docking calculations. On the basis of these considerations, site 3 was considered as not profitable to host AV analogues. Finally, also site 2 was not further considered because of its location within the intracellular compartment where the quercetin derivatives were unlikely to be delivered. Overall results from docking simulations suggested two hypothetical allosteric binding sites for AV derivatives. One of them is located within the extracellular space, while the second shows a transmembrane location.

Insulin secretion form INS-1 832/13 β-cells and primary mice islets

The functional tests were carried out using one of the most physiologically relevant in *vitro* β-cell models. In fact, we currently available, for study human insulin secretion, the INS-1 832/13 cell line, a genetically modified INS-1 cell subclone selected for its robust glucose responsiveness over the physiological range of glucose concentrations (3–23 mM glucose) retaining a differentiated cell phenotype over more than six months in culture. These characteristics made it a widely used tool for studying various aspects of β-cell function and are advantageous in a compound screening approaches. Therefore, all hybrid molecules were screened for insulin secretion. Insulin levels were measured in conditioned medium of INS-1 832/13 beta cell line treated with vehicle or various concentration (form 0 to 40 μM) of **AV**, **AV1** or **AV4** hybrid molecules by two-site immunoassay.

As shown in **Figure 6A-B**, the exposure of INS-1 832/13 cells to **AV1** molecule for 5 minutes during GSIS led to a dramatic increase of insulin secretion. The effect of **AV1** on insulin levels was dose dependent and the maximal effectiveness was found at concentration of 10 μM **AV1**, while higher doses (20-40 μM) of the compound were not able to enhance further insulin release (**Figure 6B**). No difference on insulin secretion was detected in INS-1 832/13 cells exposed to **AV** or **AV4** compounds for 5 minutes during GSIS condition (data not shown). To confirm the **AV1** secretagogue effect we performed a set of *ex-vivo* experiments using isolated mice islets as physiological model. As illustrated in **Figure 6C-D**, immune-histochemical analysis by fluorescent technique revealed that mice beta pancreatic tissue stained positively with anti-insulin antibody. A decrease of insulin immune reactivity was observed in mice islets exposed to 10 μM **AV1** for 5 minutes during GSIS experimental condition (**Figure 6D**), indicating that this hybrid molecule amplified the glucose mediated release of insulin. Quantitative analysis indicated a four-fold decrease of insulin immune reactivity in **AV1** treated mice islets compared with controls and this difference is highly significant (**Figure 6E**). Currently, the drugs used can be classified into agents that: i) enhance insulin secretion; ii) sensitize the target organs of insulin; iii) impair glucose absorption.[20] The **AV1** hybrid can fall into the first group.

Conclusion & Future Perspective

The main purpose of this paper was to identify new potential insulin modulators starting from the hypothesis that drugs able to affect glucose levels can be obtained by combining the structures of two natural and edible substances, Qu and oleic acid, through a very simple synthetic pathway. Activity results from the in *vitro* and *ex-vivo* experiments supported our strategy and derivative **AV1** clearly demonstrated to amplify the glucose mediated release of insulin, behaving as an innovative glucose level modulator. Furthermore, docking studies on **AV1** suggested for this hybrid molecule a plausible interaction with the GPR40, a GPR known in displaying a role in GSIS, and the potential binding pocket may represent an additional allosteric binding site for GPR40. Further derivatives will be synthesized to better elucidate the mechanism of action and to evaluate biological behavior in *vivo*.

Experimental

General information

All the reagents were purchased from Sigma-Aldrich or Alfa Aesar and were used as received. Organic solutions were dried over $MgSO_4$ and evaporated on a rotary evaporator under reduced pressure. Melting points were obtained using a Gallenkamp melting point apparatus. The structures

of final compounds were unambiguously assessed by ^{1}H NMR, ^{13}C NMR. ^{1}H NMR and ^{13}C NMR spectra were recorded on a Bruker 300 MHz spectrometer with TMS as an internal standard: chemical shifts are expressed in δ values (ppm) and coupling constants (*J*) in hertz (Hz). LC-MS analysis was carried out using an Agilent UHPLC instrument coupled to a QTOF mass spectrometer fitted with an electrospray ionization source (ESI) operating in positive or negative ion mode (6200 series TOF/6500 series Q-Tof B.05.01 (B5125). GC-MS analyses were performed using a 30 m × 0.25 mm, PhMesiloxane capillary column. The mass detector was operated in the electron impact ionization mode (EIMS) with an electron energy of 70 eV. Progress of the reaction was monitored by TLC on silica gel plates Merck 60 F254. Final products were purified by a flash chromatography system with column chromatography, using Merck 60 silica gel, 230-400 mesh.

*Ketal Formation - Synthesis of compound 2-(2,2-diphenylbenzo[d][1,3]dioxol-5-yl)-3,5,7-trihydroxy-4H-chromen-4-one (**AV**)*

The **AV** compound was prepared according to a described procedure**[21]** by adding to Qu (1 eq) α,α-dichlorodiphenylmethane (1 eq) without any solvent. The reaction mixture was heated at 170-180 °C under nitrogen atmosphere for 10 min. The reaction was diluted with water and extracted with ethyl acetate. The collected organic layer was washed with brine and dried. Filtration and evaporation of solvent furnished a residue that was purified by crystallization with n-hexane to afford AV as yellow crystals. Yield of **AV** 45%. Mp: 218-219 °C. The ^{1}H and ^{13}C NMR are according with those reported in literature.

*Synthesis of 2-(2,2-diphenylbenzo[d][1,3]dioxol-5-yl)-5,7-dihydroxy-4-oxo-4H-chromen-3-yl oleate (**AV1**)*

A well stirred solution of oleic acid (1 eq), *N*,*N'*-dicyclohexylcarbodiimide (DCC) (1.2 eq) and a catalytic amount of dimethylaminopyridine (DMAP) in dry dichloromethane (DCM) (2 ml) were added at 0°C, leaving the reaction mixture at that temperature for 30 minutes; then a solution of compound **AV** in dry DCM was added dropwise. The reaction mixture was stirred at 25°C, in the dark under nitrogen atmosphere, overnight. The reaction mixture was filtered on Celite® washing with DCM several times. The solvent was removed under reduced pressure, giving a residue that was purified by flash-chromatography using as eluent a mixture of *n*-hexane: ethyl acetate (7:3). The pure compound was isolated as an amorphous yellow solid, yield 58.4%. ^{1}H NMR (300 MHz, CDCl3) δ = 11.9 (br.s, 1H, **OH-C5**), 10.3 (br.s, 1H, **OH-C7**), 7.90-7.87 (m, 1H), 7.76-7.70 (m, 4H),

7.56-7.50 (m, 6H), 7.13 (d, 1H, *J* = 8.1 Hz), 6.80-6.75 (m, 1H), 6.50 (s, 1H), 6.40 (s, 1H), 4.26 (d, 2H, **CH=CH**, *J* = 7.2 Hz), 2.30-2.10 (m, 6H), 1.80-1.70 (m, 2H), 1.60-1.30 (m, 20H), 1.00 (s, 3H, **CH_3**); ^{13}C NMR (75 MHz, CDCl3) δ = 171.1, 170.1, 166.0, 164.0, 156.9, 156.0, 149.5, 149.1, 146.2, 139.1 (x2C), 138.0, 130.5, 130.2, 130.0 (x2C), 129.9 (x4C), 128.3, 127.5, 126.2, 125.4, 122.3, 107.8, 98.8, 94.2, 49.2, 48.4, 33.6 (x2C), 33.1, 31.8, 31.1 (x2C), 29.8 (x2C), 29.5 (x2C), 29.3, 28.9, 26.4, 24.9, 22.6, 14.1. GCMS (E.I.) ***m/z***: 264 $[M]^-$. ESI-MS: ***m/z*** 265 ([C11H22O7]-H)-, ***m/z*** 452 $[M]^-$.

*Synthesis of 2-(2,2-diphenylbenzo[d][1,3]dioxol-5-yl)-5-hydroxy-4-oxo-4H-chromene-3,7-diyl dioleate (**AV4**)*

It was followed the same procedure described to obtain monoester derivative, but using 2 equivalent of acyl donor (oleic acid). The residue was purified by column chromatography with n-hexane: ethyl acetate (2:1) as eluent. The pure compound was isolated as a yellow solid, yield 52.5%. Mp: 72.4 °C. ^{1}H NMR (300 MHz, CDCl3) δ = 12.22 (br. s. 1H, OH-C5), 7.66-7.55 (m, 6H), 7.47-7.37 (m, 6H), 7.06-6.97 (m, 2H), 6.3 (dd, 1H, *J* = 1.8, 8.5 Hz.),6.56 (dd, 1H, *J* = 2.0, 5.0 Hz.), 5.43- 5.20 (m, 4H, 2xCH=CH), 2.70-2.50 (m, 4H), 2.10-1.90 (m, 8H), 1.70-1.50 (m, 4H), 1.45-1.10 (m, 39H), 0.90-0.80 (m, 6H, **2xCH_3**). ^{13}C NMR (75 MHz, CDCl3) δ = 175.0, 163.8, 160.9, 157.2, 156.3, 148.7, 147.5, 145.0, 139.8, 135.6, 130.0 (x4C), 129.7, 129.3, 128.9, 128.7, 128.4, 128.3, 127.4, 126.2 (x2C), 125.3, 124.7, 122.8, 108.6 (x2C), 107.8, 103.3, 99.1, 94.1, 49.4, 33.8 (x4C), 33.1, 32.9, 31.9, 29.7 (x4C), 29.6 (x6C), 29.5, 29.3, 29.1 (x2C), 29.0, 27.2, 27.1, 25.6, 24.8, 24.3, 23.9, 22.6, 14.1 (x2C).

Computational details

The structure of ligands was submitted to the LigPrep routine (implemented in Maestro 9.2 within the Schrödinger Suite 2011),**[22]** using OPLS_2005 as the force field and Epik 2.2 to generate possible tautomers at pH 7 ± 2. The structure of GPR40 (resolution 2.33 Å, protein data bank entry 4phu)[2], was refined by means of the Protein Preparation Wizard to add hydrogens, assign bond orders, and sample water molecule orientation. SiteMap 2.5, with default settings, was then applied to identify potential ligand binding sites on GPR40. Next, Glide 5.7 was used to perform docking calculations on GPR40 ligands. A distinct receptor grid was generated for each potential binding site identified in the previous step. Grid size was adjusted manually to best fit shape and size of each site. Rotation of all receptor hydroxyl groups contained within the gridbox was allowed during grid generation. Root mean square deviation was calculated for the crystallographic structure of both TAK-875 and the oleoyl glycerol in comparison to the best docked pose and was found less

than 1 Å in both cases, thus suggesting the ability of Glide in handling such structural systems and the reliability of docking calculations.

Cell Culture. Pancreatic β-cell line INS-1 832/13 (provided by Prof. C. Newgard, Duke University, Durham, USA) were used. Insulin secreting INS-1 832/13 cells, stably transfected with a plasmid coding for human Proinsulin, were maintained in RPMI-1640 medium supplemented with 10% fetal bovine serum, 10 mM HEPES, 2 mM L-glutamine, 1 mM sodium pyruvate, 50 mM β-mercaptoethanol, 100 IU/ml penicillin, and 100 IU/ml streptomycin. Cells were incubated under 95% O_2, 5% CO_2 at 37 °C. Media were refreshed every 2-3 days and cells were trypsinized and passaged weekly. Cells were subcultured when they approached ≥70% confluence.

Insulin Secretion Detection

$5x10^5$ INS-1 832/13 β-cells were plated in 24 wells plates with RPMI 1640 11 mM Glucose, 10% FBS. The next day, the media was switched to 5 mM Glucose, 10 % FBS. After 16 hours incubation, β-cells were washed and secretion medium (HBSS with 20 mM Hepes and 1% BSA, pH 7.2) was added containing 3 mM glucose. After 2 h, secretion medium was replaced with fresh secretion medium containing 3 or 23 mM glucose with or without Qu, oleic acid, AV and AV 1-4 at different concentrations and different minutes of incubation time. Levels of insulin in cell media, of three independent experiment in duplicate, were detected by insulin ELISA kit (Calbiotech Inc) according to manufacturer's instructions. Briefly, the media was spun 5 minutes at 2.500 rpm, 4°C, to pellet down cellular debris and either immediately assayed or frozen in liquid N_2 first and -80°C successively, for no longer than a week.

Islet isolation

Islets were isolated from adult male C57/BL6 mice, weighing 36 ± 2 g (Charles River, Calco, Como, Italy), as described by Montana et al.**[23]** Briefly, pancreas was digested with 10 ml of PBS solution containing 5 mg/mL of collagenase (type P; Boehringer Mannheim, Mannheim, Germany). The pancreas was dissected and incubated in a stationary water bath at 37°C for 25 minutes. After digestion, the islets were separated on a density gradient (Histopaque-1077; Sigma, St Louis, MO, USA) and placed into a flask overnight. The day after islets were transferred and handpicked under microscope observation. Islets were cultured for 24 h in RPMI containing 11.1 mmol/l glucose supplemented with 10% FCS, penicillin (100 U/ml) and streptomycin (100 µg/ml) in standard humidified culture conditions of 5% CO_2 and 95% air at 37°C prior to GSIS.

Islets staining

Islets are cytospun onto gelatin-coated slides. After a 5-minute fixing step in 2% paraformaldehyde in PBS, slides are blocked with 10% normal donkey serum blocking solution (Jackson Immunoresearch) for 1 hour at room temperature. Samples were incubated with a primary anti-insulin antibody (1:200, Dako) overnight at 4 °C, followed by three 5-min washes in PBS. Dylight 488 secondary Ab (Jackson Immunoresearch) incubation was done for 1 h at room temperature. Slides are washed 3 times and coverslips mounted with antifade mounting medium with DAPI (Life Technologies). Images are viewed at 40x magnification and captured with Leica AF6000 microscope (Leica Wetzlar, Germany)

Statistical analysis

Statistical differences were determined by one-way analysis of variance (ANOVA) followed by Dunnet's Multiple Comparison Test and the results were expressed as mean +/- SD from n independent experiments. Differences were considered statistically significant for $P<0.05$.

Financial & competing interests disclosure

The authors have no relevant affiliations or financial involvement with any organization or entity with a financial interest in or financial conflict with the subject matter or materials discussed in the manuscript. This includes employment, consultancies, honoraria, stock ownership or options, expert testimony, grants or patents received or pending, or royalties. No writing assistance was utilized in the production of this manuscript.

Executive Summary

Type 2 Diabetes Mellitus

Type 2 Diabetes Mellitus represents a social problem, which is treated with several side effects and complications.

Nature offers a remedy

Natural polyphenols and fatty acids are interesting substances with multiple biological and chemical properties.

Chemistry and Molecular Docking

Two oleoyl derivatives of Quercetin have been synthesized as monoester and diester. 2-(2,2-diphenylbenzo[d][1,3]dioxol-5-yl)-5,7-dihydroxy-4-oxo-4H-chromen-3-yl oleate (**AV1**) was docked on GPR40, identifying an allosteric binding site. It could be useful for a rational design of safe and effective antidiabetic agents.

***In vitro* and *ex vivo* experiments**

Glucose-Stimulated Insulin Secretion was interfered by **AV1** in a dose-dependent manner in INS-1 832/13 β-cells; it is also demonstrated in male C57/BL6 mice islets.

References

[1] Vasapollo P, Cione E, Luciani F, Gallelli L, *Curr Drug Saf* doi: 10.2174/1574886311666160405110515 (2016).

[2] Perri M, Caroleo MC, Liu N *et al. Exp. Cell. Res.* doi: 10.1016/j.yexcr.2017.03.022 (2017).

[3] Rutter GA, Pullen TJ, Hodson DJ, Martinez-Sanchez A, *Biochem. J.* 466(2), 203-218 (2015).

[4] Sharma G, Prossnitz ER, *Endocrinology* 152(8), 3030-3039 (2011).

[5] Ferdaoussi M, Bergeron V, Zarrouki B *et al. Diabetologia* 55(10), 2682-2692 (2012).

[6] McKillop AM, Moran BM, Abdel-Wahab YHA, Flatt PR, *Br J Pharmacol.* 170(5), 978-990 (2013).

[7] Liu B, Hassan Z, Amisten S *et al. Diabetologia* 56(11), 2467-2476 (2013).

[8] Carullo G, Cappello AR, Frattaruolo L, Badolato M, Armentano B, Aiello F, *Future Med. Chem.* 9(1), 79-93 (2017).

[9] Bardy G, Virsolvy A, Quignard JF *et al. Br J Pharmacol.* 169(5), 1102-1113 (2013).

[10] Mukhopadhyay P, Prajapati AK, *RSC Adv.* 5, 97547-97562 (2015).

[11] Chen C, Li H, Long Y, *Bioorg. Med. Chem. Lett*. 26(23), 5603–5612 (2016).

[12] Lin DCH, Guo Q, Luo *et al.* J, *Mol. Pharm.* 82, 843-859 (2012).

[13] Srivastava A, Yano J, Hirozane Y *et al. Nature* 513, 124-127 (2014).

[14] Tikhonova IG, Poerio E, *BMC Struct. Biol. 15*,16 (2015).

[15] Fujiwara K, Maekawa F, Yada T, *Am J Physiol Endocrinol Metab* 289(4), E670-E677 (2005).

[16] Hohmeier HE, Mulder H, Chen G, Henkel-Rieger R, Prentki M, Newgard CB, *Diabetes* 49(3), 424-430 (2000)

[17] Hectors TLM, Vanparys C, Pereira-Fernandes A, Martens GA, Blust R, *PLoS One* 8(3), e60030 (2013).

[18] Kane MA, Folias AE, Pingitore A *et al. PNAS* 107(50), 21884-21889 (2010).

[19] Maini F, Contini A, Nava D *et al. J Am Oil Chem Soc* 90, 1751-1759 (2013).

[20] Röder PV, Wu B, Liu Y, Han W, *Exp Mol Med* 48, e219 (2016).

[21] Li N, Shi Z, Tang Y, Yang J, Duan J, *Beilstein J. Org. Chem.* 5, 60 (2009).

[22] Schrödinger, LLC, http://www.schrodinger.com

[23] Montana E, Bonner-Weir S, Weir GC. *J. Clin. Invest.* 91, 780 (1993).

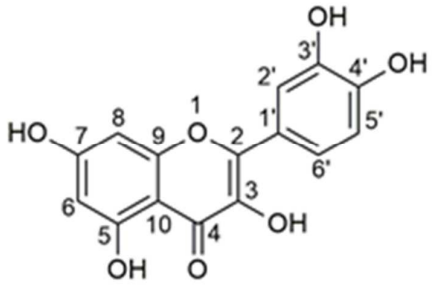

Figure 1. Quercetin

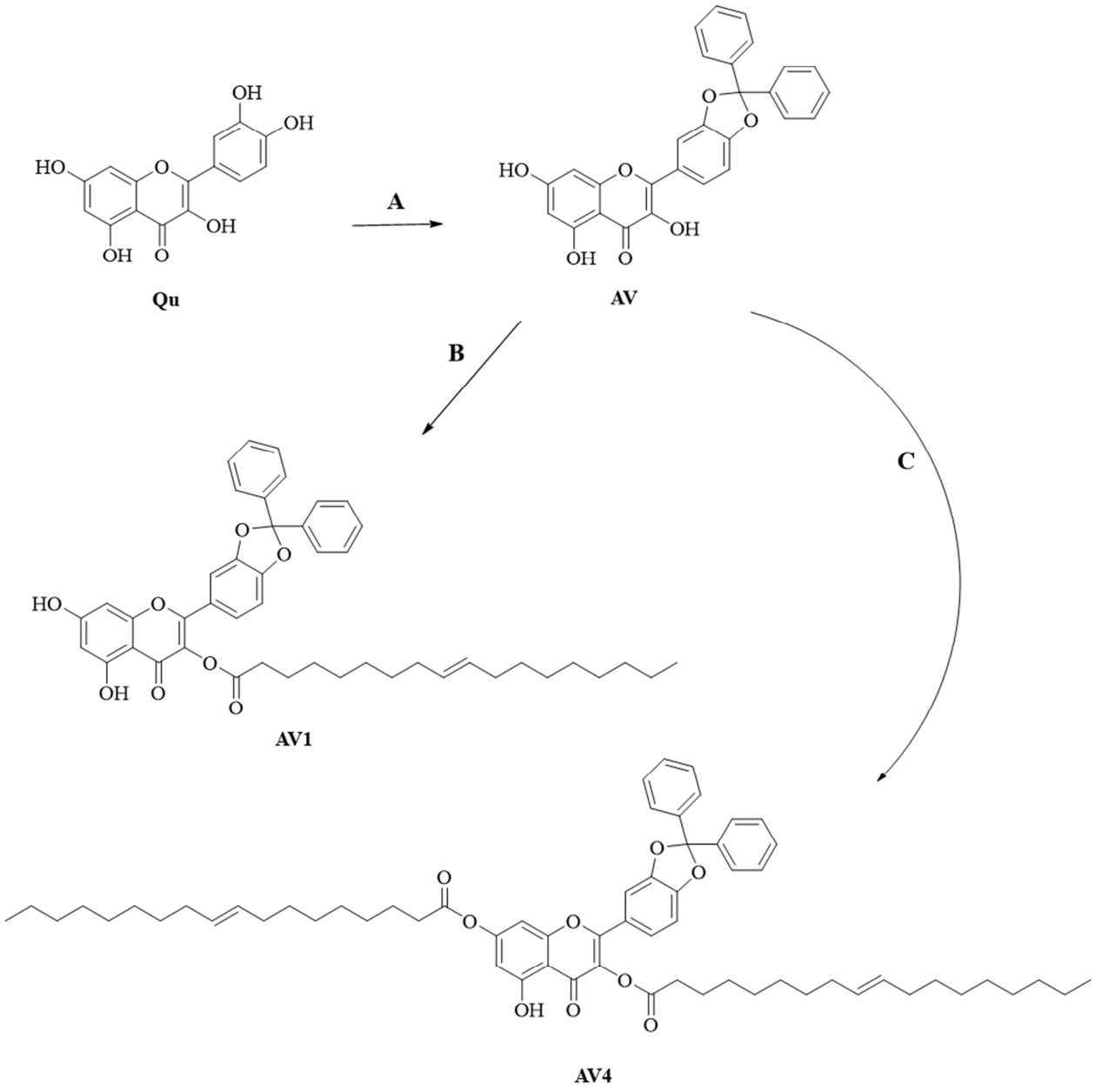

Figure 2. A) Reagents and conditions: α,α-dichlorodiphenylmethane, 170-180°C, 10 min. **B,C**) Oleic acid (as acyl donor), *N*,*N'*-dicyclohexylcarbodiimide (DCC), Dimethylaminopyridine (DMAP) in dry dichloromethane at 0°C for 30 min., then AV solution in dry dichloromethane was added dropwise, 25 °C, overnight under nitrogen atmosphere. *Oleic acid molar ratio*: 1 equivalent for **B**, 2 equivalents for **C**.

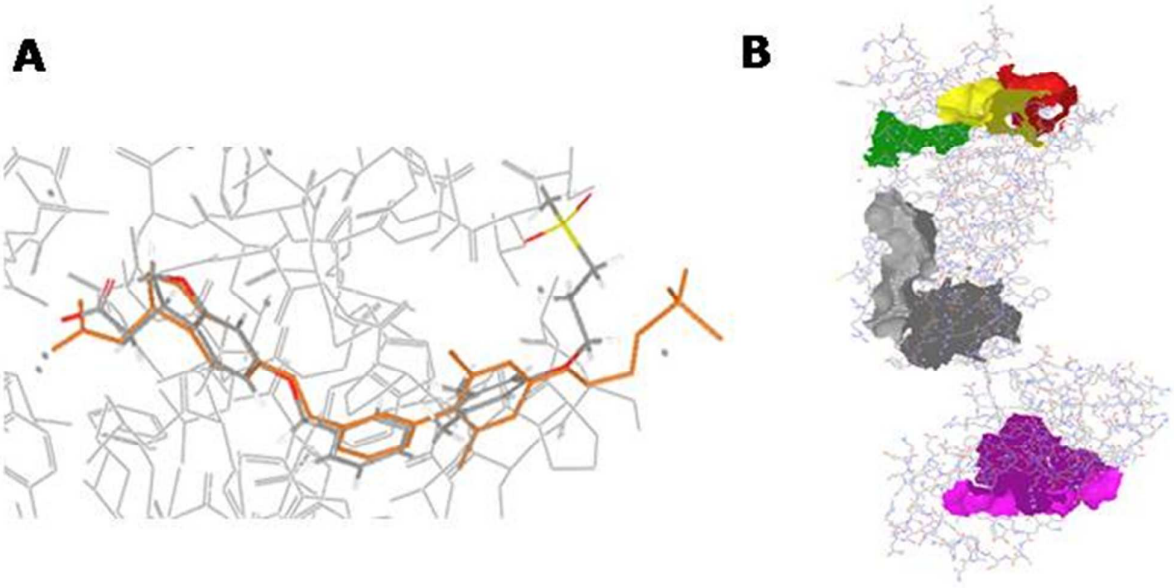

Figure 3. **A**) Superposition of the crystallographic structure of TAK-875 (orange) with the corresponding best docked conformation (atom type notation). A very similar binding mode is shown, apart the sulfonyl side chain exposed to the solvent that is free to rotate. **B**) Hypothetical binding sites identified by the SiteMap routine on the GPR40 structure. Site 3 (green) accommodates the allosteric agonist TAK875, as well as the oleoyl-glycerol is embedded within site 2 (gray) in the X-ray crystallographic structure. Two additional small and globular sites (site 4, red, and site 5, yellow) are located in proximity of the extracellular side. Finally, site 2 (magenta) is found within the cytoplasmic side of the GPR40 structure.

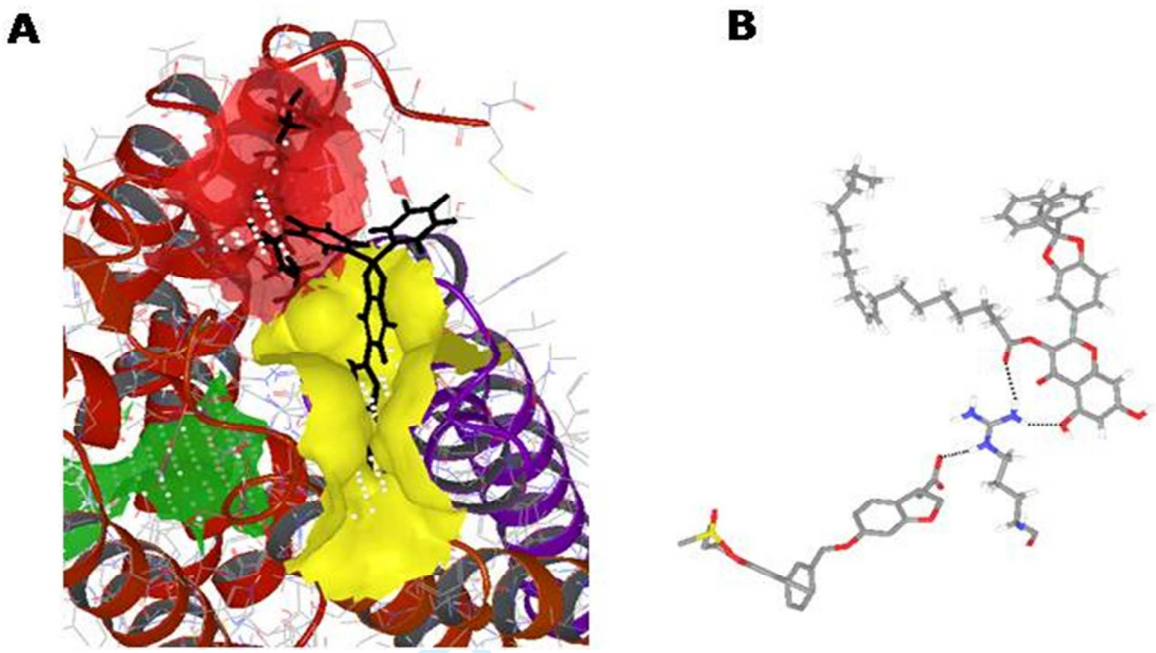

Figure 4. A) Hypothetical binding mode of AV1 within the pocket resulting from merging of site 4 (red) and site 5 (yellow). The alkyl portion of the ligand is located within site 4, while the quercetin moiety fulfills site 5. Importantly, site 5 is adjacent to site 3 (green, that accommodates TAK-875) and they are separated by Arg183, known to be one of the most important amino acids required to anchor the carboxyl group of allosteric agonists, such as TAK-875. **B**) Hypothetical interaction pattern involving TAK-875 within its allosteric binding site as derived from X-ray crystallography (lower left corner), AV1 within the predicted binding site resulting from merging of site 4 and 5, and their interactions with Arg183, one of the most important amino acids required for anchoring the carboxylic function of allosteric agonists of GPR40.

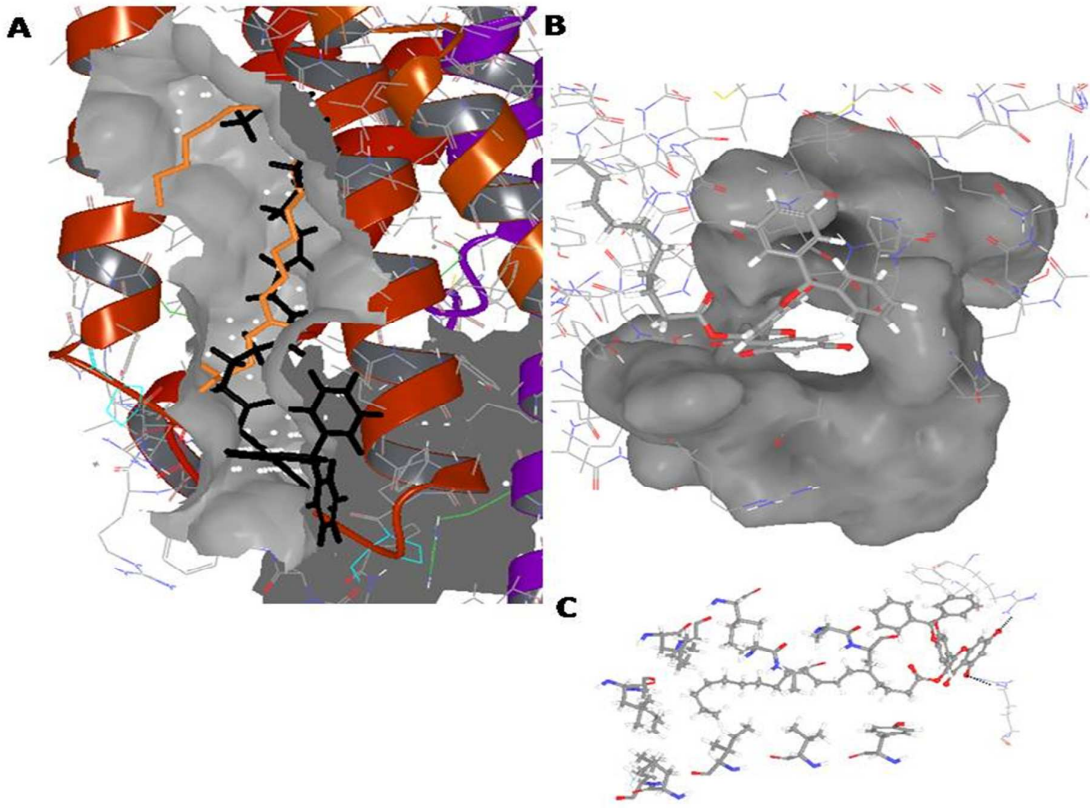

Figure 5. Schematic representation of the interaction pattern between AV1 and site 1 on GPR40**. A**) Comparison of the binding pose of AV1 (black) to the oleyl-glicerol derivative (orange) of the crystallographic structure. Site 1 is located between TM4 and TM5 (left and right, respectively), while TM3 is behind the ligand. **B**) The condensed phenyl ring of the quercetin core of AV1 is accommodated within site 1 in such a way that the hydroxyl group at position 7 is directed toward a tunnel that points to the opposite face of the GPR40 structure. **C**) The alkyl chain of the ligand (ball and stick notation) is embedded within hydrophobic residues (stick notation) belonging to both TM4 (left) and TM5 (right). The hydroxyl groups at positions 5 and 7 are involved in a bifurcated hydrogen bond (black dotted lines) with Arg37 (line notation, lower left corner) and in a simple hydrogen bond with Arg218 (line notation, lower right corner). A π-π stacking is also found between the ketal moiety of the ligand and the phenyl ring of Phe110.

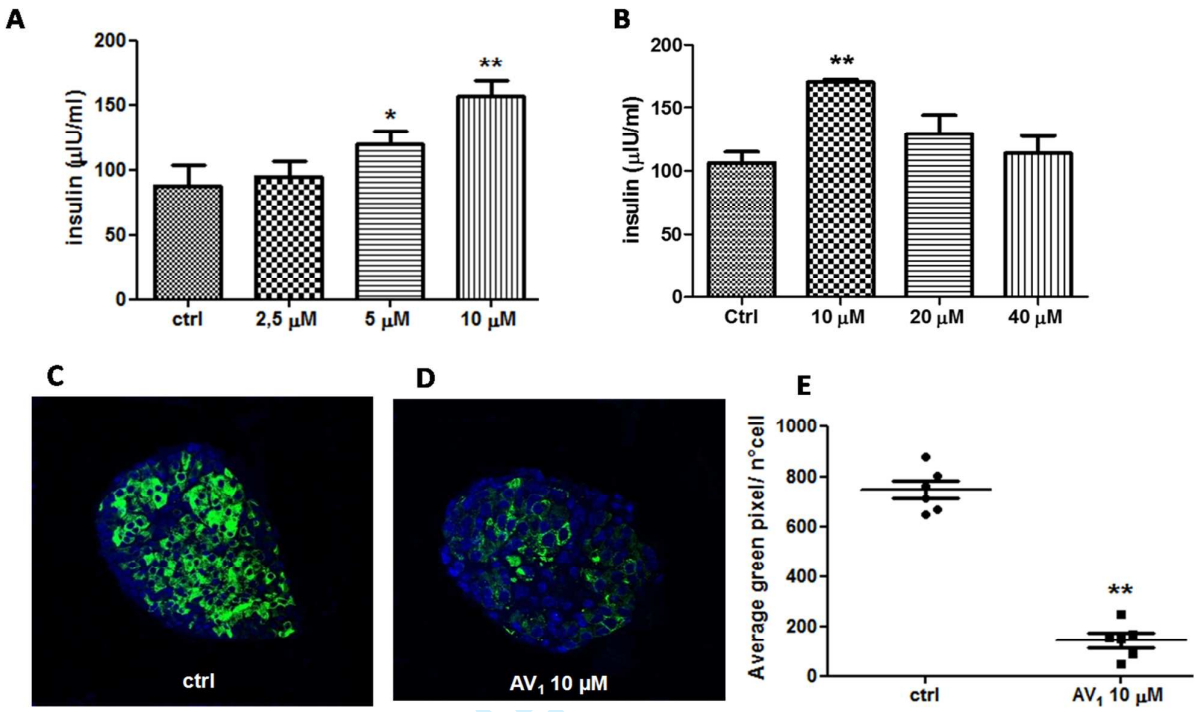

Figure 6. Insulin secretion from INS-1 832/13 β-cells and primary islets culture. **A** and **B**) Pancreatic INS-1 832/13 β-cells were treated with different concentration of AV1 (0-10 µM) for 5 minutes during GSIS condition. Insulin quantification was determined by ELISA technique. (*p<0.05 and **p<0.001 one-way ANOVA followed by Dunnet's Multiple Comparison Test, as post hoc), (n=3). **C**) Insulin immunostaining of isolated islets from adult male C57/BL6 mice, treated with DMSO (as vehicle) or **D**) AV1 10 µM. Figures are representative of three independent experiments. **E**) Average green pixel immunostaining analysis (**p<0.001 one-way ANOVA followed by Dunnet's Multiple Comparison Test, as post hoc).